

Minimization of the positional errors for an accurate determination of the kinematic parameters of a rigid-body system with miniature inertial sensors

Jurij Žumer^a, Janko Slavič^a, Miha Boltežar^{a,*}

^aUniversity of Ljubljana, Faculty of Mechanical Engineering, Aškerčeva 6, SI-1000 Ljubljana, Slovenia

Cite as:

Žumer, Jurij, Janko Slavič, and Miha Boltežar. "Minimization of the positional errors for an accurate determination of the kinematic parameters of a rigid-body system with miniature inertial sensors." *Mechanism and Machine Theory* 81 (2014): 193-208.

DOI: 10.1016/j.mechmachtheory.2014.07.008

<http://www.sciencedirect.com/science/article/pii/S0094114X14001840>

Abstract

This paper presents an approach to minimize and control the error of the kinematic parameters of the space-constraint rigid-body system by using inertial micro-electro-mechanical sensors (MEMS). We analyze the error propagation when the kinematic joint constraints are observed for a sensor-fusion update in the kinematic model because of the uncertain position of the inertial sensors. The minimization of the errors of the kinematic parameters comes from applying multiple inertial units on every rigid body with the controlled input positional error between each inertial unit. The analytical approach proposes the inclusion of the position vectors from the inertial units to the kinematical joints into the state vector that consists of the observed kinematical and sensor parameters. A Kalman-filtering procedure is used to observe the state vector and, additionally, the adaptive estimation of the position vectors from the inertial units to the kinematic joints or constraints is presented in order to achieve the optimum performance of the filter. The analytical approach is experimentally validated on a pendulum mechanism, where the improved performance of the proposed approach is confirmed.

Keywords: rigid-body system, kinematic joint, accelerometer, gyroscope, sensor fusion, error minimization

1. Introduction

Control over the kinematics of a rigid-body system, such as an industrial mechanism, is essential in engineering practice. On the one hand, the kinematic parameters of the observed system can be analytically defined, but this procedure might be time consuming because of the complexity of

*Corresponding author

Email address: miha.boltezar@fs.uni-lj.si (Miha Boltežar)

the system, and furthermore, obtaining information about the exact external forces over time is usually not straightforward if the system is not kinematically driven. On the other hand, the experimental observation and control of the kinematic parameters is a strongly competitive approach, especially if the parameters must be observed or controlled at a later stage. These experimental procedures are possible with inertial MEMS sensors, which in the past decade have begun to offer an alternative to traditional inertial sensors, or other appropriate devices, such as encoders and optical systems. The advantages of MEMS are a small weight and size and an attractive price, while their disadvantages relate to their long-term stability and accuracy, which become crucial during an integration procedure over time.

To control the long-term precision of experimentally defined kinematic parameters researchers have used aiding systems to update the inertial parameters. The fusion of different systems largely depends on the observed application. In the field of biomechanics Roetenberg [1, 2] and Schepers [3, 4] presented extensive research on combining the magnetic and inertial principle for an orientation determination of the human body. In industrial environments the use of the magnetic principle might be critical because of the interference with local magnetic fields or because of the ferromagnetic materials of the mechanisms, despite the proposed calibration procedures. Furthermore, the use of the magnetic and inertial principles shows reduced precision when the human body is exposed to increased translational and rotational accelerations because of the loosely-coupled constraints between the parts of the human body and the environment, as was shown by Brodie [5]. Therefore, other aiding systems were combined, such as a satellite signal [5, 6], like in car navigation [7]. Also, in the field of biomechanics and entertainment the inertial principle is combined with an optical system [8, 9], especially for an orientation determination, and with the UWB-RF system [10] for positioning purposes. However, the disadvantage of these aiding systems is more expensive hardware in comparison to the inertial MEMS sensors, the possibility of their installation in mechanisms in a robust industrial environment and the inaccessibility of the aiding signal. Therefore, the correction of the inertial principle in the case of a rigid-body mechanism should primarily rely on the constraints in the kinematic joints as much as possible.

A more specific approach to the observation of the kinematic parameters of the mechanisms was presented by Wagner [11]. He observed the independent degrees of freedom of the mechanism with the inertial principle and then corrected the calculated positions of the bodies and the inertial parameters with aiding radar units. However, his approach still requires more detailed knowledge of the observed kinematics and is therefore time consuming. Cheng [12] made a survey of the approaches to measuring the relative angles between coupled rigid bodies on a human body and a robotic mechanism using only inertial sensors. The observed methods differ in the type of inertial sensors used, in their number and in their layout on every body. Besides the lack of accuracy when using gyroscopes over a long period of time, Cheng highlighted the reduced angular accuracy due to the uncertain positioning of the accelerometers, which is problematic during fast rotations. He confirmed, on a simple mechanism, that the best solution is obtained when two accelerometers with a known distance and without any gyroscopes on each rigid body are used. However, in order to observe the position and velocity conditions the relations between the rigid bodies of the observed system must again be known in detail.

The observation of the kinematic parameters of the rigid-body system using inertial MEMS sensors is therefore challenged by the use of the appropriate aiding systems or kinematic con-

straints and by the precise positioning of the inertial units. The following research, in contrast to [1–11], focuses on the rigid-body mechanism problem, where only kinematic constraints are available for the long-term control of the kinematic and inertial parameters. Furthermore, in contrast to [11] and [12] we propose a general approach to the simultaneous characterization of the kinematic parameters with no need to inspect the independent and dependent degrees of freedom using a Kalman-filter formulation. Consequently, the expected uncertain estimation of the position vectors from the inertial units to the kinematic joints in everyday engineering practice might cause inaccuracy or the divergent behavior of the filter. Therefore, we present a solution by applying multiple inertial units on each rigid body with controlled positional errors between each other, which is based on the deduction of the error-propagation analysis in kinematic joints.

In the following Sec. 2 the inertial positioning is overviewed. The error propagation of the kinematic-constraints update is investigated and the conclusion for the use of the multiple inertial unit on each rigid body is presented. Sec. 3 presents a general formulation of the state and observation vector for a rigid-body system in a Kalman filter with the included adaptive estimation of the position vectors from the inertial units to the kinematic joints for optimum filter performance. Finally, in Sec. 4 the experimental validation is presented on a two-body pendulum mechanism to confirm the improved accuracy of the kinematic parameters.

2. Error-propagation analysis of the observation constraints in kinematic joints

2.1. Inertial positioning overview

The position \mathbf{r}^i , velocity \mathbf{v}^i and the orientation \mathbf{q}^i at an arbitrary point O^i on the i^{th} -body, expressed in the reference frame $x^n y^n z^n$ as shown in Fig. 1, are, in discrete form, calculated from the raw acceleration $\bar{\mathbf{a}}^{s,i}$, the raw angular rate $\bar{\boldsymbol{\omega}}^{s,i}$, the accelerometer bias \mathbf{b}_a^i and the gyroscope bias \mathbf{b}_ω^i , expressed in the i^{th} -frame, as:

$$\mathbf{r}_{k+1}^i = \mathbf{r}_k^i + \mathbf{v}_k^i \Delta t, \quad (1)$$

$$\mathbf{v}_{k+1}^i = \mathbf{v}_k^i + \left(\mathbf{A}_k^i \left(\bar{\mathbf{a}}_k^{s,i} - \mathbf{b}_{a,k}^i \right) + \mathbf{g} \right) \Delta t, \quad (2)$$

$$\mathbf{q}_{k+1}^i = \mathbf{q}_k^i + \frac{1}{2} \mathbf{q}_k^i \otimes \left(\tilde{\boldsymbol{\omega}}_k^{s,i} - \tilde{\mathbf{b}}_{\omega,k}^i \right) \Delta t. \quad (3)$$

\mathbf{A}^i is the transformation matrix from the i^{th} -frame to the reference frame, \mathbf{g} is the gravity vector and Δt is the time interval between the successive time steps k and $k+1$. The symbol \otimes represents the quaternion product and the symbol $\tilde{}$ represents a vector in quaternion form. The quaternion algebra and the related transformations are clearly presented in [13]. Considering the Eqs. (2) and (3), the true acceleration $\bar{\mathbf{a}}^i$ and the true angular rate $\bar{\boldsymbol{\omega}}^i$ in the i^{th} -frame are defined as:

$$\bar{\mathbf{a}}^i = \bar{\mathbf{a}}^{s,i} - \mathbf{b}_a^i, \quad (4)$$

$$\bar{\boldsymbol{\omega}}^i = \bar{\boldsymbol{\omega}}^{s,i} - \mathbf{b}_\omega^i. \quad (5)$$

The bias values of the MEMS sensors change over time, mostly because of the variation of the surrounding temperature and because of their stochastic behavior. Choukroun [14] modeled the

bias values as constants; however, the identification of the stochastic parameters in the time domain using the Allan variance [15, 16] shows that the long-term changing of the bias can be modeled as the exponentially correlated Gauss-Markov process [17]. This approach of the stochastic modeling at the same time satisfies the condition of the normally distributed noise if the sensor bias is observed within the state vector in the Kalman filter. Furthermore, because it is hard to distinguish and separate different sources in practice, Gebre [18] showed that the Gauss-Markov model can also be efficient when the temperature changes slowly in the surrounding environment. Following the latter approach, the bias vectors \mathbf{b}_a and \mathbf{b}_ω can be written in discrete form as [19]:

$$\mathbf{b}_{a,k+1}^i = \mathbf{b}_{a,k}^i e^{-\beta_a^i \Delta t}, \quad (6)$$

$$\mathbf{b}_{\omega,k+1}^i = \mathbf{b}_{\omega,k}^i e^{-\beta_\omega^i \Delta t}, \quad (7)$$

where the components of the bias vectors β_a^i and β_ω^i stand for the inverse values of the correlation times $\tau_{c,a}^i$ and $\tau_{c,\omega}^i$ of the accelerometer and the gyroscope, respectively.

2.2. Error-propagation analysis in kinematic joints

The error of the kinematic parameters increases rapidly during the integration procedure over time if Eqs. (1)-(7) are used in a straightforward manner. If only the kinematic constraints are considered within the Kalman-filter formulation to minimize this error, the rigid-body system should fulfill the conditions that each rigid body needs at least one kinematic relation to the other bodies and at least one rigid body in the system must have a kinematic relation to the environment. In another case an additional aiding system should be used. However, the accuracy of the kinematic constraints, such as the position and velocity conditions in kinematic joints, also has an influence on the efficiency of the Kalman filter.

Assuming the arbitrary l^{th} -kinematic joint between the i^{th} - and j^{th} -body in Fig. 1, the position vector \mathbf{r}_c^l and the velocity \mathbf{v}_c^l at the point C^l can be written with respect to the i^{th} -body:

$$\mathbf{r}_c^l = \mathbf{r}^i + \mathbf{A}^i \bar{\mathbf{u}}^i, \quad (8)$$

$$\mathbf{v}_c^l = \mathbf{v}^i + \mathbf{A}^i (\bar{\boldsymbol{\omega}}^i \times \bar{\mathbf{u}}^i), \quad (9)$$

where $\bar{\mathbf{u}}^i$ represents the position vector from the inertial unit on the i^{th} -body to the kinematic joint C^l , expressed in the i^{th} -body frame. Analogously, Eqs. (8) and (9) can be written with the respect to the j^{th} -body. The position vector $\bar{\mathbf{u}}^i$ is estimated when the inertial unit is fixed to the body and is assumed to be constant in the following deduction. The opposite case will be discussed later in the text. The error propagation of the position vector $\delta \mathbf{r}_c^l$ and the velocity $\delta \mathbf{v}_c^l$ can be deduced with the total differentiation of Eqs. (8) and (9). Additionally, we must consider the following equality [13]:

$$\mathbf{A}\{\mathbf{q} + \delta \mathbf{q}\} = \mathbf{A}(\mathbf{I} + \delta \boldsymbol{\phi}^\times), \quad (10)$$

that describes the change of the transformation matrix \mathbf{A} because of the orientation change $\delta \mathbf{q}$. $\delta \boldsymbol{\phi}^\times$ is a skew-symmetric matrix of the vector $\boldsymbol{\phi}$, which represents the imaginary vector part of the quaternion change $\delta \mathbf{q}$. It follows that:

$$\delta \mathbf{r}_c^l = \delta \mathbf{r}^i - \mathbf{A}^i (\bar{\mathbf{u}}^i)^\times \delta \boldsymbol{\phi}^i + \mathbf{A}^i \delta \bar{\mathbf{u}}^i, \quad (11)$$

$$\delta \mathbf{v}_c^l = \delta \mathbf{v}^i - \mathbf{A}^i (\bar{\boldsymbol{\omega}}^i \times \bar{\mathbf{u}}^i)^\times \delta \boldsymbol{\phi}^i - \mathbf{A}^i (\bar{\mathbf{u}}^i)^\times \delta \bar{\boldsymbol{\omega}}^i + \mathbf{A}^i (\bar{\boldsymbol{\omega}}^i)^\times \delta \bar{\mathbf{u}}^i, \quad (12)$$

where \times stands for the skew-symmetric matrix of the observed vector. Analyzing Eqs. (11) and (12) the errors $\delta \mathbf{r}^i$, $\delta \mathbf{v}^i$, $\delta \boldsymbol{\phi}^i$ and the angular rate error $\delta \bar{\boldsymbol{\omega}}^i$, which can be simplified to the error of the gyroscope bias $\delta \mathbf{b}_\omega^i$, represent the group of errors that are related to the estimated position, velocity, quaternion and bias parameter for the i^{th} -body described by Eqs. (1)-(3) and (7). If these parameters are observed within the state vector in the Kalman filter, using the theory of [19], their errors should be normally distributed and their mean values should be equal to zero.

The remaining error $\delta \bar{\mathbf{u}}^i$ is the error of the estimated position vector $\bar{\mathbf{u}}^i$. This error mechanism cannot be assumed to be normally distributed, because it is hard to achieve the accuracy of the position vector $\bar{\mathbf{u}}^i$ to the level of the measurement-tool accuracy in everyday practice. Such a case could be the exact position of the accelerometer, which is hidden inside the inertial unit. Further, the accessibility to the kinematic joints could be reduced and consequently, the position vectors could only be estimated. Furthermore, the measurement tool could have inadequate accuracy. Therefore, the error vector $\delta \bar{\mathbf{u}}^i$ can only have an initial estimation. However, if the error mechanism, which has an influence on the observation constraint, is not normally distributed there might be inferior performance from the Kalman filter, which can also lead to a divergence.

Therefore, an accurate estimation of the position vectors from the inertial units to the kinematic joints represents an important step toward an accurate estimation of the kinematic parameters. In the following step the procedure for minimizing this error will be deduced. Fig. 2 presents the same arbitrary rigid bodies with the kinematic joint as Fig. 1, with the difference being that there is an arbitrary number of inertial units on each body. Consider the position vector \mathbf{u}_{mn}^i between the m^{th} -unit and n^{th} -unit on the i^{th} -body, expressed in the reference frame:

$$\mathbf{r}_n^i - \mathbf{r}_m^i = \mathbf{u}_{mn}^i. \quad (13)$$

In addition, the following relation can be written regarding the equality of the description of the position vector $\mathbf{r}_c^l = \mathbf{r}_{c,m}^l = \mathbf{r}_{c,n}^l$ of the kinematic joint C^l with respect to the m^{th} -unit and the n^{th} -unit on the i^{th} -body:

$$\mathbf{r}_{c,n}^l - \mathbf{r}_{c,m}^l = \mathbf{r}_n^i + \mathbf{u}_n^{l,i} - \mathbf{r}_m^i - \mathbf{u}_m^{l,i} = \mathbf{r}_n^i + \mathbf{A}_n^i \bar{\mathbf{u}}_n^{l,i} - \mathbf{r}_m^i - \mathbf{A}_m^i \bar{\mathbf{u}}_m^{l,i} = \mathbf{0}, \quad (14)$$

where $\mathbf{u}_m^{l,i}$ and $\mathbf{u}_n^{l,i}$ represent the position vectors from the m^{th} -unit and the n^{th} -unit on the i^{th} -body to the arbitrary l^{th} -kinematic joint. The $\bar{}$ above these vectors indicates that they are expressed in the local sensor frames. Furthermore, considering Eqs. (13) and (14) it is possible to show the following relation:

$$\mathbf{u}_m^{l,i} - \mathbf{u}_n^{l,i} = \mathbf{u}_{mn}^i. \quad (15)$$

Finally, the error propagation of the position vector $\delta \mathbf{r}_{c,m}^l$ and the velocity vector $\delta \mathbf{v}_{c,m}^l$ of the l -kinematic joint with respect to the i^{th} -body can be written with a consideration of Eq. (15):

$$\delta \mathbf{r}_{c,m}^l = \delta \mathbf{r}_m^i - \mathbf{A}_m^i (\bar{\mathbf{u}}_m^{l,i})^\times \delta \boldsymbol{\phi}_m^i + (\delta \mathbf{u}_n^{l,i} + \delta \mathbf{u}_{mn}^i), \quad (16)$$

$$\delta \mathbf{v}_{c,m}^l = \delta \mathbf{v}_m^i - \mathbf{A}_m^i (\bar{\boldsymbol{\omega}}_m^i \times \bar{\mathbf{u}}_m^{l,i})^\times \delta \boldsymbol{\phi}_m^i - \mathbf{A}_m^i (\bar{\mathbf{u}}_m^{l,i})^\times \delta \bar{\boldsymbol{\omega}}_m^i + (\boldsymbol{\omega}_m^i)^\times (\delta \mathbf{u}_n^{l,i} + \delta \mathbf{u}_{mn}^i), \quad (17)$$

where $\boldsymbol{\omega}_m$ represents the angular rate of the m^{th} -unit expressed in the reference frame. Analogously, we can write the error propagation of the position vector $\delta \mathbf{r}_{c,n}^l$ and the velocity vector $\delta \mathbf{v}_{c,n}^l$ of the

l^{th} -kinematic joint. However, in Eqs. (12) and (13) there is another error mechanism $\delta \mathbf{u}_{mn}^i$, which is related to the error of the position vector between the m^{th} and n^{th} -units. In contrast to the errors $\delta \mathbf{u}_m^{l,i}$ and $\delta \mathbf{u}_n^{l,i}$, the amplitude of $\delta \mathbf{u}_{mn}^i$ can be minimized if the position vector \mathbf{u}_{mn}^i is controlled when the inertial units are placed on the rigid body. This action is possible in practice with a planned allocation of inertial units. $\delta \mathbf{u}_{mn}^i$ can be minimized to the accuracy level, which is negligible compared to the amplitude of the bodies' movement. If the described assumption is fulfilled, the position vectors from the inertial units to the kinematic constraints can be estimated together with the kinematic and sensor parameters within the state vector in the Kalman filter, because the position vectors between the inertial units, such as \mathbf{u}_{mn}^i , represent the additional positional constraints.

3. Formulation of the kinematic model

3.1. Process model

In general, the kinematic parameters described with Eqs. (1)-(5) can be observed at every point on the arbitrary i^{th} -body, where the inertial units are attached. However, while the position and velocity vectors differ between each other during the motion in these points, the orientation of the i^{th} -body remains the same. Therefore, in order to reduce the number of sensors on every body, the arbitrary n number of inertial units actually represents the n number of accelerometers and only one gyroscope. If the angular rate is measured at the m^{th} -unit, then the state vector \mathbf{x}^i of the kinematic and sensor parameters on the i^{th} -body can be written as:

$$\begin{aligned} \mathbf{x}^i &= \left((\mathbf{r}_1^i)^T, (\mathbf{v}_1^i)^T, (\mathbf{b}_{a,1}^i)^T, \dots, (\mathbf{r}_m^i)^T, (\mathbf{v}_m^i)^T, (\mathbf{b}_{a,m}^i)^T, \dots, (\mathbf{q}_m^i)^T, (\mathbf{b}_{\omega,m}^i)^T \right)^T = \\ &= \left((\mathbf{x}_1^i)^T, \dots, (\mathbf{x}_m^i)^T, \dots, (\mathbf{q}_m^i)^T, (\mathbf{b}_{\omega,m}^i)^T \right)^T. \end{aligned} \quad (18)$$

If the system consists of n rigid bodies, then the state vector \mathbf{x} of all the observed kinematic and sensors parameters is:

$$\mathbf{x} = \left((\mathbf{x}^1)^T, \dots, (\mathbf{x}^i)^T, \dots, (\mathbf{x}^n)^T \right)^T \quad (19)$$

Considering the assumption of observing the position vectors from the inertial units to the kinematic joints, a state vector \mathbf{x}_u can be additionally written:

$$\mathbf{x}_u = \left((\bar{\mathbf{u}}_1^{1,1})^T, \dots, (\bar{\mathbf{u}}_m^{l,i})^T, \dots \right)^T. \quad (20)$$

These position vectors are modeled as constants; therefore, the arbitrary position vector $\bar{\mathbf{u}}_m^{l,i}$ from the m^{th} -inertial unit on the i^{th} -body to the l^{th} -kinematic joint between two successive time steps is calculated as:

$$\bar{\mathbf{u}}_{m,k+1}^{l,i} = \bar{\mathbf{u}}_{m,k}^{l,i}. \quad (21)$$

Finally, all the observed parameters are joined in the state vector \mathbf{x}_{kin} :

$$\mathbf{x}_{kin} = \left(\mathbf{x}^T, \mathbf{x}_u^T \right)^T. \quad (22)$$

The nonlinear relation between the two successive observation steps of the state vector \mathbf{x}_{kin} describes a function \mathbf{f}_{kin} :

$$\mathbf{x}_{kin,k+1} = \mathbf{f}_{kin}(\mathbf{x}_{kin,k}, \bar{\mathbf{a}}_{1,k}^{s,1}, \bar{\omega}_{1,k}^{s,1}, \dots, \bar{\mathbf{a}}_{m,k}^{s,i}, \bar{\omega}_{m,k}^{s,i}, \dots) + \mathbf{w}_k \quad (23)$$

where \mathbf{w}_k represents the process noise with the covariance matrix $\mathbf{Q}_{kin} = \begin{bmatrix} \mathbf{Q} & \mathbf{0} \\ \mathbf{0} & \mathbf{Q}_u \end{bmatrix} = E[\mathbf{w}_k \mathbf{w}_k^T]$.

Because the parameters of the state vector \mathbf{x}_{kin} have nonlinear relations, the extended Kalman filter (EKF) is used in this study with the total formulation [20]. Therefore, the state transition matrix Φ_k in k -th step is defined as:

$$\Phi_k(\mathbf{x}_{kin,k}) = \frac{\partial \mathbf{f}_{kin}(\mathbf{x}_{kin,k})}{\partial \mathbf{x}_{kin}}. \quad (24)$$

The details of the Kalman filter, followed by this research, are discussed elsewhere [14, 18, 19].

3.2. Observation model

Observing the kinematic constraints between the rigid bodies and the position vectors between the inertial units on every rigid body, three types of observation equation can be defined:

1. Observation of the kinematic constraints: The number of these constraints depends on the number and the types of the kinematic joints. In general, the mathematical description of these joints, such as spherical, cylindrical, translational joint, etc., are discussed in details by Shabana in [21]. Regarding the parameters in the state vector \mathbf{x} the positional constraint equations \mathbf{h}_{cr} , the velocity constraint equations \mathbf{h}_{cv} and the orientational constraint equations $\mathbf{h}_{c\phi}$ should be defined if they are possible. For the arbitrary l^{th} -kinematic joint the constraints are joined in the observation vector \mathbf{y}_c^l :

$$\mathbf{y}_c^l = \mathbf{h}_c^l(\mathbf{x}_{kin}) = \begin{pmatrix} \mathbf{h}_{cr}^l(\mathbf{x}_{kin}) \\ \mathbf{h}_{cv}^l(\mathbf{x}_{kin}) \\ \mathbf{h}_{c\phi}^l(\mathbf{x}_{kin}) \end{pmatrix} = \mathbf{0}. \quad (25)$$

For the rigid-body system all the available kinematic constraints are joined in the following observation vector:

$$\mathbf{y}_c = \mathbf{h}_c(\mathbf{x}_{kin}) = \left((\mathbf{h}_c^1)^T, \dots, (\mathbf{h}_c^l)^T, \dots \right)^T = \mathbf{0}, \quad (26)$$

2. Observation of the kinematic parameters at different positions on every rigid body: These observations relate to Eq. (13). Because the inertial values are primarily expressed in the local coordinate systems of the inertial units, we first write the transformation matrix \mathbf{A}_{mn} that describes the relation between the local coordinate systems of the arbitrary m^{th} - and n^{th} -inertial units:

$$\mathbf{A}_n^i = \mathbf{A}_m^i \mathbf{A}_{mn}^i, \quad (27)$$

The transformation matrix \mathbf{A}_{mn} is constant if the inertial units are fixed on the rigid body. Assuming the observation in the coordinate system of the m^{th} -inertial unit, the positional and

velocity constraints in the vector $\mathbf{y}_{l,mn}^i$ can be defined between the origin of the m^{th} - and the n^{th} -inertial units on the i^{th} -body, based on the known position vector \mathbf{u}_{mn}^i , which is written as $\bar{\mathbf{u}}_{m,mn}^i$ in the m^{th} -coordinate system:

$$\mathbf{y}_{l,mn}^i = \mathbf{h}_{l,mn}^i(\mathbf{x}_m^i, \mathbf{x}_n^i, \bar{\mathbf{u}}_{m,mn}^i) = \begin{pmatrix} \mathbf{r}_n^i - \mathbf{r}_m^i - \mathbf{A}_m^i \bar{\mathbf{u}}_{m,mn}^i \\ \mathbf{v}_n^i - \mathbf{v}_m^i - \mathbf{A}_m^i (\bar{\boldsymbol{\omega}}_m^i \times \bar{\mathbf{u}}_{m,mn}^i) \end{pmatrix} = \mathbf{0}. \quad (28)$$

Observing the whole system the observation vector \mathbf{y}_l can be written as:

$$\mathbf{y}_l = \mathbf{h}_l(\mathbf{x}) = ((\mathbf{y}_{l,12}^1)^T, \dots, (\mathbf{y}_{l,mn}^i)^T, \dots)^T = \mathbf{0}. \quad (29)$$

3. Observation of the position vectors from the inertial units to the kinematic joints: The third group of observation equations comes from Eq. (15). Observing the position vectors from the arbitrary m^{th} - and n^{th} -inertial units on the i^{th} -body to the l^{th} -kinematic joint, the observation vector $\mathbf{y}_{u,mn}^{l,i}$ is:

$$\mathbf{y}_{u,mn}^{l,i} = \mathbf{h}_{u,mn}^{l,i}(\bar{\mathbf{u}}_m^{l,i}, \bar{\mathbf{u}}_n^{l,i}, \bar{\mathbf{u}}_{m,mn}^i) = \bar{\mathbf{u}}_m^{l,i} - \mathbf{A}_{mn}^i \bar{\mathbf{u}}_n^{l,i} - \bar{\mathbf{u}}_{m,mn}^i = \mathbf{0}. \quad (30)$$

Regarding all the difference vectors on all the rigid bodies, the observation vector \mathbf{y}_u is defined as:

$$\mathbf{y}_u = \mathbf{h}_u(\mathbf{x}_u) = ((\mathbf{y}_{u,12}^{1,1})^T, \dots, (\mathbf{y}_{u,mn}^{l,i})^T, \dots)^T = \mathbf{0}. \quad (31)$$

The second and third groups of the observation equations can be defined because of the use of the multiple inertial units on every rigid body and, consequently, they represent the additional conditions for the correction of the kinematic parameters within the state vector \mathbf{x}_{kin} . All three groups of observations are grouped into the observation vector \mathbf{y} :

$$\mathbf{y} = \mathbf{h}(\mathbf{x}_{kin}) = (\mathbf{y}_c^T, \mathbf{y}_l^T, \mathbf{y}_u^T)^T. \quad (32)$$

The matrix \mathbf{H} represents the relation between the predicted state $\hat{\mathbf{x}}_{kin}^-$ and the observations at the linearization point of the function \mathbf{h} and is defined as:

$$\mathbf{H} = \begin{bmatrix} \mathbf{H}_c \\ \mathbf{H}_l \\ \mathbf{H}_u \end{bmatrix} = \begin{bmatrix} \frac{\partial \mathbf{h}_c}{\partial \mathbf{x}_{kin}} \\ \frac{\partial \mathbf{h}_l}{\partial \mathbf{x}_{kin}} \\ \frac{\partial \mathbf{h}_u}{\partial \mathbf{x}_{kin}} \end{bmatrix}. \quad (33)$$

The covariance matrix \mathbf{R} of the normally distributed observation deviations is also divided into three parts:

$$\mathbf{R} = \begin{bmatrix} \mathbf{R}_c & \mathbf{0} & \mathbf{0} \\ \mathbf{0} & \mathbf{R}_l & \mathbf{0} \\ \mathbf{0} & \mathbf{0} & \mathbf{R}_u \end{bmatrix}. \quad (34)$$

The covariance matrix \mathbf{R}_c in practice depends on the tightness conditions in the joints, while the covariance matrices \mathbf{R}_l and \mathbf{R}_u depend on the accuracy of the allocation of the inertial units between each other on every rigid body. The part of \mathbf{R}_l that relates to the velocity observations, also depends on the normally distributed angular rate noise. Consequently, the expected deviation in the kinematic joints and the accuracy of the inertial unit positioning also influence the accuracy of the observed state vector \mathbf{x}_{kin} .

3.3. Adaptive estimation of the joint position vectors

The initial estimation of the covariance matrix \mathbf{Q}_u describes the initial, normally distributed deviations of the position vectors from the inertial units to the kinematic joints. If the position vectors in \mathbf{x}_u converge to the exact values, then the values of the covariance matrix \mathbf{Q}_u should decrease over time. For the optimum operation of the Kalman filter the covariance matrix \mathbf{Q}_u must be adjusted with respect to the estimated deviation of the position vectors in \mathbf{x}_u .

The deviation of the state vector \mathbf{x}_u can be estimated in every k^{th} -step of the Kalman filter when the predicted vector $\widehat{\mathbf{x}}_{u,k+1}^-$ is compared to the observation vector $\mathbf{y}_{u,k+1}$:

$$\Delta \mathbf{y}_{u,k+1} = \mathbf{y}_{u,k+1} - \mathbf{H}_{u,k+1} \widehat{\mathbf{x}}_{u,k+1}^-, \quad (35)$$

where $\Delta \mathbf{y}_{u,k+1}$ represents the residual error of the position vectors from the inertial units to the kinematic joints. If the state vector \mathbf{x}_u converges to the true value, the covariance matrix \mathbf{Q}_u must be adjusted in such a way that the residual error $\Delta \mathbf{y}_{u,k+1}$ is minimized. In this study the minimization process follows the approach in [14] and is adapted for the estimation of the state vector \mathbf{x}_u .

For every pair of position vectors $\mathbf{u}_m^{l,i}$ and $\mathbf{u}_n^{l,i}$ on the i^{th} -body the minimization equation $J(\mu^i)$ can be written [14]:

$$J(\mu^i) = |\Delta \mathbf{y}_{u,k+1}^i (\Delta \mathbf{y}_{u,k+1}^i)^T - \mathbf{S}_{k+1}^{i-} (\mu^i)|^2, \quad (36)$$

where $|\cdot|$ stands for the Frobenius norm of the observed matrix. Vector $\Delta \mathbf{y}_{u,k+1}^i$ consists of all the residual errors that can be determined on the i^{th} -body using arbitrary $\mathbf{y}_{u,mn}^{l,i}$ vectors:

$$\Delta \mathbf{y}_{u,k+1}^i = \begin{pmatrix} \Delta \mathbf{y}_{u,12,k+1}^{l,i} \\ \vdots \\ \Delta \mathbf{y}_{u,mn,k+1}^{l,i} \\ \vdots \end{pmatrix}. \quad (37)$$

\mathbf{S}_{k+1}^{i-} represents the part of the Kalman gain factor \mathbf{S}_{k+1}^- that relates to the covariance matrix of the residual error $\Delta \mathbf{y}_{u,k+1}^i$. \mathbf{S}_{k+1}^- follows as [14]:

$$\mathbf{S}_{k+1}^- = \left(\mathbf{H}_{k+1} \mathbf{P}_{k+1}^- \mathbf{H}_{k+1}^T + \mathbf{R}_{k+1} \right)^{-1}. \quad (38)$$

μ^i is a minimization factor for the adjustment of the covariance matrix \mathbf{Q}_u at the position of the subcovariance matrices $\mathbf{Q}_{u,1}^i, \dots, \mathbf{Q}_{u,m}^i, \dots$ on the i^{th} -rigid body. It is deduced in [14] that the factor μ^i is defined as:

$$\mu^i = \frac{\text{tr}(\Delta \mathbf{y}_{u,k+1}^i (\Delta \mathbf{y}_{u,k+1}^i)^T - \mathbf{N}_1) \mathbf{L}_1^T}{\text{tr}(\mathbf{L}_1 \mathbf{L}_1^T)} \quad (39)$$

and

$$\mu^i = \begin{cases} \mu^i; & \mu^i > 0 \\ 0; & \mu^i \leq 0 \end{cases}. \quad (40)$$

The components N_1 and L_1 in Eq. (34) are calculated as follows [14]:

$$N_1 = \mathbf{H}_{u,k+1}^* \mathbf{I} \mathbf{H}_{u,k+1}^{*T}, \quad (41)$$

$$L_1 = \mathbf{H}_{u,k+1}^* \mathbf{P}_{k+1}^* \mathbf{H}_{u,k+1}^{*T} + \mathbf{R}_{k+1}^*. \quad (42)$$

The matrices $\mathbf{H}_{u,k+1}^*$, \mathbf{P}_k^* and \mathbf{R}_{k+1}^* represent the parts of the matrices $\mathbf{H}_{u,k+1}$, \mathbf{P}_{k+1}^- and \mathbf{R}_{k+1} in the Kalman filter that relate to the position vectors from the inertial units to the kinematic joints on the i^{th} -body:

$$\mathbf{H}_{u,k+1}^* = \begin{bmatrix} \mathbf{H}_{u,12,k+1}^{l,i} \\ \vdots \\ \mathbf{H}_{u,mn,k+1}^{l,i} \\ \vdots \end{bmatrix}, \quad (43)$$

$$\mathbf{P}_{k+1}^* = \begin{bmatrix} \mathbf{P}_{u_1^i,k+1}^- & \cdots & \cdots & \mathbf{0} \\ \vdots & \ddots & & \vdots \\ \vdots & & \mathbf{P}_{u_m^i,k+1}^- & \vdots \\ \mathbf{0} & \cdots & \cdots & \ddots \end{bmatrix}, \quad (44)$$

$$\mathbf{R}_{k+1}^* = \begin{bmatrix} \mathbf{R}_{u,12,k+1}^{l,i} & \cdots & \cdots & \mathbf{0} \\ \vdots & \ddots & & \vdots \\ \vdots & & \mathbf{R}_{u,mn,k+1}^{l,i} & \vdots \\ \mathbf{0} & \cdots & \cdots & \ddots \end{bmatrix}. \quad (45)$$

When the coefficient μ^i is determined, the adapted covariance matrices of the position vectors from the inertial units to the arbitrary l^{th} -kinematic joint on the arbitrary i^{th} -body are:

$$\mathbf{Q}_{u,1}^{l,i} = \dots = \mathbf{Q}_{u,m}^{l,i} = \dots = \mu^i \mathbf{I}. \quad (46)$$

3.4. Discussion on the kinematic model

The presented kinematic model is deduced generally for the multiple inertial units on every rigid body with controlled position vectors between the inertial units. Fig. 3 summarize the application of the proposed process and the observation model within the Kalman-filtering iteration. However, the use of the multiple inertial units on every rigid body would result in unnecessary costs and processing power, especially if large systems would be observed. Therefore, the presented approach would follow the simplification of the use of only two inertial units on every rigid body, because in this case the condition of the controlled position vectors is also satisfied. The selection of the same number of accelerometers was also made in practice by Cheng [12], where he showed an improved performance of the angle determination at lower rotation speeds.

In Sec. 2.2 we consider the constant position vectors from the inertial units to the kinematic joints. However, the presented approach should not differ if these position vectors are time dependent, because we showed in Sec. 3.1 that they are included in the state vector \mathbf{x}_{kin} . On the other hand, the advantage of the constant position vectors from the inertial units to the kinematic joints is the possibility of their elimination from state vector \mathbf{x}_{kin} , when they converge to the real values.

4. Experimental validation

4.1. Experimental set-up

The experimental validation of the developed model was made on a two-degrees-of-freedom (DoF) pendulum. Fig. 5(a) presents the scheme of the pendulum, which consists of two equal ($l_b^1 = l_b^2$) 0.8-meter-long block rods, while Fig. 5(b) shows the set-up in the laboratory. In the system of two rigid bodies ($i = \{1, 2\}$) there are two rotational joints ($l = \{1, 2\}$). The first joint connects the pendulum to the fixed base and the second joint connects the rigid bodies. The origin of the reference coordinate system $x^n y^n z^n$ is in the center of the first rotational joint, where y^n is oriented in the opposite direction to the acceleration due to gravity \mathbf{g} with accuracy of 0.5° . Next, we continue to the deduction in Sec. 3.4 and we use two inertial units on every body ($m = \{1, 2\}$). In the resting position, the local coordinate systems of the inertial unit have the same orientation as the reference coordinate system.

The measurement of accelerations and angular rates was made with the miniature inertial units CH-6d that consists of a tri-axis $\pm 3g$ accelerometer ADXL335, a two-axis $\pm 400^\circ/\text{s}$ gyroscope LPR510ALH and a single-axis $\pm 400^\circ/\text{s}$ gyroscope LY510ALH. The enlarged figure of one of the inertial units on the pendulum is presented in Fig 6(a). The deterministic parameters of the sensors, such as the sensitivity and bias values, were determined with the autocalibration procedures. The calibration of the accelerometers follows the method presented by Frosio [22] and the calibration of the gyroscopes follows the procedure described by Syed [23]. On the other hand, the stochastic parameters of the sensors for the determination of the covariance matrix \mathbf{Q} were determined after a 24-hour test in the resting position at a controlled temperature of 25° with the Allan deviation procedure as described in [17].

Two 12-bit absolute encoders Contelec Vert-X28 with an accuracy of 0.1° were used as a reference system for the observation of the relative angles in the joints and, consequently, for the calculation of the other kinematic parameters. They were fixed in the rotational joints, as shown in Fig. 6(b) for the second joint between the first and the second body.

According to the proposed indexation of the position vectors from the inertial units to the kinematic joints in Sec. 2, and with the help of Fig. 5(a), the following vectors stand for the pendulum:

$$\begin{aligned} \bar{\mathbf{u}}_1^{1,1} &= (0, 0.15, 0)^T \text{m}, & \bar{\mathbf{u}}_2^{1,1} &= (0, 0.65, 0)^T \text{m}, & \bar{\mathbf{u}}_1^{2,1} &= (0, -0.648, 0)^T \text{m}, \\ \bar{\mathbf{u}}_2^{2,1} &= (0, -0.148, 0)^T \text{m}, & \bar{\mathbf{u}}_1^{2,2} &= (0, 0.15, 0)^T \text{m}, & \bar{\mathbf{u}}_2^{2,2} &= (0, 0.65, 0)^T \text{m}. \end{aligned} \quad (47)$$

Consequently, the difference of the position vectors between the inertial units on each rigid body using Eq. (15) are:

$$\bar{\mathbf{u}}_{12}^1 = (0, -0.5, 0)^T \text{m}, \quad \bar{\mathbf{u}}_{12}^2 = (0, -0.5, 0)^T \text{m}. \quad (48)$$

The numerical values of the position vectors in Eq. (47) will be used as the reference values for the observed position vectors, while the vectors $\bar{\mathbf{u}}_{12}^1$ and $\bar{\mathbf{u}}_{12}^2$ will be used in the observation part of the Kalman filter. For the purposes of the experimental validation the accuracy of the positioning of the inertial units was within 0.4 millimeters. However, in order to simulate the inaccurate positioning of the inertial units, the initial error was set for the position vectors in Eq. (47) with a standard deviation of 2.5 centimeters, which represents an error of 3% of the length of every rod. This value was also used for building the initial covariance matrix \mathbf{Q}_u .

According to Eq. (27) the initial difference in the orientation of the inertial units must be determined despite the fact that the positioning of the inertial units on each rigid body is controlled. Using the comparison of the response of the calibrated accelerometers in different static positions, the matrices \mathbf{A}_{12}^1 and \mathbf{A}_{12}^2 can be defined using the least-squares method. For the case of the proposed experiment these matrices are functions of the following Euler angles with the zyx successive rotations [21]:

$$\Theta_{12}^1 = (0.36^\circ, -0.4^\circ, 0.81^\circ)^T, \quad \Theta_{12}^2 = (0.54^\circ, 0.02^\circ, -0.45^\circ)^T. \quad (49)$$

For the experimental validation we proposed a combination of the different motion regimes. From the initial resting position, the pendulum was forced into accelerated motion. During the motion the pendulum was exposed to accelerations and decelerations until it swung back to the initial position. The motion was observed for approximately six minutes. For reasons of clarity, Fig. 7(a) presents the change of the absolute angle in the rotational joint with respect to the reference frame in the first minute of motion, while Fig. 7(b) presents the change of the absolute angle in the last minute, when the pendulum swung down.

4.2. Kinematic model of a 2-DoF pendulum

For the observed 2-DoF pendulum, according to Eq. (18) the state vectors \mathbf{x}^1 and \mathbf{x}^2 that describe the kinematic and sensor parameters for the first and second rigid bodies can be defined as:

$$\mathbf{x}^1 = \left((\mathbf{r}_1^1)^T, (\mathbf{v}_1^1)^T, (\mathbf{b}_{a,1}^1)^T, (\mathbf{r}_2^1)^T, (\mathbf{v}_2^1)^T, (\mathbf{b}_{b,2}^1)^T, (\mathbf{q}_I^1)^T, (\mathbf{b}_\omega^1)^T \right)^T, \quad (50)$$

$$\mathbf{x}^2 = \left((\mathbf{r}_1^2)^T, (\mathbf{v}_1^2)^T, (\mathbf{b}_{a,1}^2)^T, (\mathbf{r}_2^2)^T, (\mathbf{v}_2^2)^T, (\mathbf{b}_{b,2}^2)^T, (\mathbf{q}_I^2)^T, (\mathbf{b}_\omega^2)^T \right)^T, \quad (51)$$

As shown in Fig. 5(a), the state vector \mathbf{x}_u of the position vectors to the kinematic constraints for the observed pendulum can be written considering Eq. (20):

$$\mathbf{x}_u = \left((\bar{\mathbf{u}}_1^{1,1})^T, (\bar{\mathbf{u}}_2^{1,1})^T, (\bar{\mathbf{u}}_1^{2,1})^T, (\bar{\mathbf{u}}_2^{2,1})^T, (\bar{\mathbf{u}}_1^{2,2})^T, (\bar{\mathbf{u}}_2^{2,2})^T \right)^T. \quad (52)$$

Using Eqs. (22) the state vector \mathbf{x}_{kin} of the kinematic model is therefore:

$$\mathbf{x}_{kin} = \left((\mathbf{x}^1)^T, (\mathbf{x}^2)^T, \mathbf{x}_u^T \right)^T. \quad (53)$$

Furthermore, the observation vector \mathbf{y} in Eq. (32) follows to the separation on three parts. The vector of kinematic constraints \mathbf{y}_c in the kinematic joints regarding Eq. (26) is defined as:

$$\mathbf{y}_c = \left((\mathbf{h}_{cr}^1)^T, (\mathbf{h}_{cv}^1)^T, (\mathbf{h}_{c\phi,1}^1)^T, (\mathbf{h}_{c\phi,2}^1)^T, (\mathbf{h}_{cr}^2)^T, (\mathbf{h}_{cv}^2)^T, (\mathbf{h}_{c\phi,1}^2)^T, (\mathbf{h}_{c\phi,2}^2)^T \right)^T =$$

$$= \begin{pmatrix} \mathbf{r}_1^1 + \mathbf{r}_2^1 + \mathbf{A}^1 (\bar{\mathbf{u}}_1^{1,1} + \mathbf{A}_{12}^1 \bar{\mathbf{u}}_2^{1,1}) \\ \mathbf{v}_1^1 + \mathbf{v}_2^1 + \mathbf{A}^1 (\bar{\boldsymbol{\omega}}^{1 \times} (\bar{\mathbf{u}}_1^{1,1} + \mathbf{A}_{12}^1 \bar{\mathbf{u}}_2^{1,1})) \\ (\mathbf{e}_z^n)^T (\mathbf{A}^1 \mathbf{e}_{x_1}^1) \\ (\mathbf{e}_z^n)^T (\mathbf{A}^1 \mathbf{e}_{y_1}^1) \\ \mathbf{r}_1^1 + \mathbf{r}_2^1 + \mathbf{A}^1 (\bar{\mathbf{u}}_1^{2,1} + \mathbf{A}_{12}^1 \bar{\mathbf{u}}_2^{2,1}) - \mathbf{r}_1^2 - \mathbf{r}_2^2 - \mathbf{A}^2 (\bar{\mathbf{u}}_1^{2,2} + \mathbf{A}_{12}^2 \bar{\mathbf{u}}_2^{2,2}) \\ \mathbf{v}_1^1 + \mathbf{v}_2^1 + \mathbf{A}^1 (\bar{\boldsymbol{\omega}}^{1 \times} (\bar{\mathbf{u}}_1^{2,1} + \mathbf{A}_{12}^1 \bar{\mathbf{u}}_2^{2,1})) - \mathbf{v}_1^2 - \mathbf{v}_2^2 - \mathbf{A}^2 (\bar{\boldsymbol{\omega}}^{2 \times} (\bar{\mathbf{u}}_1^{2,2} + \mathbf{A}_{12}^2 \bar{\mathbf{u}}_2^{2,2})) \\ (\mathbf{e}_z^n)^T (\mathbf{A}^2 \mathbf{e}_{x_1}^2) \\ (\mathbf{e}_z^n)^T (\mathbf{A}^2 \mathbf{e}_{y_1}^2) \end{pmatrix} = \mathbf{0}, \quad (54)$$

where \mathbf{h}_{cr}^1 represents the positional constraints in the rotational joint between the base and the first rod. Two independent constraints with respect to the first and second inertial frames on the first body:

$$\mathbf{r}_1^1 + \mathbf{A}^1 \bar{\mathbf{u}}_1^{1,1} = \mathbf{0}, \quad \mathbf{r}_2^1 + \mathbf{A}^1 \mathbf{A}_{12}^1 \bar{\mathbf{u}}_2^{1,1} = \mathbf{0} \quad (55)$$

are simplified in one equation to minimize the total number of equations. Similarly, the function \mathbf{h}_{cv} represents the velocity constraints in the first joint, while \mathbf{h}_{cr}^2 and \mathbf{h}_{cv}^2 stand for the positional and velocity constraints in the second joint. The functions $\mathbf{h}_{c\phi,1}^1$, $\mathbf{h}_{c\phi,2}^1$, $\mathbf{h}_{c\phi,1}^2$ and $\mathbf{h}_{c\phi,2}^2$ stand for the constraints that are related only to the rotational joint. The rotation is available only around the z^n -axis in the reference frame. These constraints are not dependent on the positional and velocity constraints; therefore, they are written with the unity vectors \mathbf{e}_z^n , $\mathbf{e}_{x_1}^1$, $\mathbf{e}_{y_1}^1$, $\mathbf{e}_{x_1}^2$ and $\mathbf{e}_{y_1}^2$, which are expressed in the appropriate coordinate frames.

The observation vector \mathbf{y}_I with respect to Eq. (29) is defined as:

$$\mathbf{y}_I = \begin{pmatrix} \mathbf{h}_{I,12}^1(\mathbf{x}^1, \bar{\mathbf{u}}_{1,12}^1) \\ \mathbf{h}_{I,12}^2(\mathbf{x}^2, \bar{\mathbf{u}}_{1,12}^2) \end{pmatrix} = \begin{pmatrix} \mathbf{r}_2^1 - \mathbf{r}_1^1 - \mathbf{A}^1 \bar{\mathbf{u}}_{1,12}^1 \\ \mathbf{v}_2^1 - \mathbf{v}_1^1 - \mathbf{A}^1 ((\bar{\boldsymbol{\omega}}^1)^\times \bar{\mathbf{u}}_{1,12}^1) \\ \mathbf{r}_2^2 - \mathbf{r}_1^2 - \mathbf{A}^2 \bar{\mathbf{u}}_{1,12}^2 \\ \mathbf{v}_2^2 - \mathbf{v}_1^2 - \mathbf{A}^2 ((\bar{\boldsymbol{\omega}}^2)^\times \bar{\mathbf{u}}_{1,12}^2) \end{pmatrix} = \mathbf{0}, \quad (56)$$

and finally, the observation vector \mathbf{y}_u with respect to Eq. (31) follows as:

$$\mathbf{y}_u = \begin{pmatrix} \mathbf{h}_{u,12}^{1,1}(\bar{\mathbf{u}}_1^{1,1}, \bar{\mathbf{u}}_2^{1,1}, \bar{\mathbf{u}}_{1,12}^1) \\ \mathbf{h}_{u,12}^{2,1}(\bar{\mathbf{u}}_1^{2,1}, \bar{\mathbf{u}}_2^{2,1}, \bar{\mathbf{u}}_{1,12}^1) \\ \mathbf{h}_{u,12}^{2,2}(\bar{\mathbf{u}}_1^{2,2}, \bar{\mathbf{u}}_2^{2,2}, \bar{\mathbf{u}}_{1,12}^2) \end{pmatrix} = \begin{pmatrix} \bar{\mathbf{u}}_1^{1,1} - \mathbf{A}_{12}^1 \bar{\mathbf{u}}_2^{1,1} - \bar{\mathbf{u}}_{1,12}^1 \\ \bar{\mathbf{u}}_1^{2,1} - \mathbf{A}_{12}^1 \bar{\mathbf{u}}_2^{2,1} - \bar{\mathbf{u}}_{1,12}^1 \\ \bar{\mathbf{u}}_1^{2,2} - \mathbf{A}_{12}^2 \bar{\mathbf{u}}_2^{2,2} - \bar{\mathbf{u}}_{1,12}^2 \end{pmatrix} = \mathbf{0}. \quad (57)$$

The covariance matrix \mathbf{R} using Eqs. (34) was defined according to the expected deviations in the kinematic constraints. The covariance matrix \mathbf{R}_c depends on the tightness in the joint bearings. Because of the tight connection the positional deviation was set to 0.1 millimeter. Furthermore, the positional deviations in the covariance matrices \mathbf{R}_I and \mathbf{R}_u depend on the accuracy of the measurement tool or on the accuracy of the positioning procedure between inertial units. In this study, the deviation was found to be 0.4 millimeter. On the other hand, the deviations of the velocity constraints depend mainly on the normally distributed noise in the angular rate data. The orientational constraints were limited to a 0.1° deviation.

4.3. Analysis of the experimental results

In the experimental analysis the presented adaptive Kalman formulation with the estimation of the position vectors from the inertial units to the kinematic joints (KF1) will be compared with the formulation that does not consider the estimation of the position vectors from the inertial units to the kinematic joints in the state vector \mathbf{x}_{kin} (KF2). However, the results calculated straightforwardly from the inertial data will not be presented because the errors increase enormously in a few seconds.

In the first step the errors of the kinematic parameters are examined. Fig. 8 presents the absolute error value of the position vector \mathbf{r}_1^1 on the first body and of the position vector \mathbf{r}_2^2 on the second body, expressed in the reference frame. The results show the minimized and steady errors of the

position vectors when the KF1 formulation with the adaptive estimation is used. In contrast, the KF2 formulation also shows steady, but higher, absolute errors. These errors are the consequence of the inaccurate initial estimation of the position vectors from the inertial units to the kinematic joints and, furthermore, they influence the assumption of the Kalman filter that the error of the observation vector y_c is normally distributed with the zero mean value. A larger deviation of the position vector r_2^2 is related to the fact that this inertial unit has the greatest distance from the base of the pendulum. Therefore, when the pendulum is accelerated or decelerated, a possible movement in the z^n -axis can reduce the performance of the filter. When the pendulum swung down the error also decreases. Regarding the size of the pendulum in Fig. 5 and the large angle changes over time in Fig. 7, the constant error under 2% shows the appropriate approach when using the adaptive formulation.

Fig. 9 shows the absolute error of the velocity vectors v_1^1 on the first body and v_2^2 on the second body in the reference frame. The KF1 formulation shows better or equivalent results compared to the KF2 formulation. However, there is a clear difference in the error values when the pendulum is in the resting position or when it moves between 10 and 250 seconds. The difference can be related to the noise in the angular rate data, which affects the observations in Eqs. (54) and (56). However, the absolute errors are consistently under 2%, which again supports the use of the proposed adaptive filter.

Another kinematic parameter is the orientations of the rigid bodies. Fig. 10 presents the absolute angle error around the z^n -axis in the reference frame. The angle is calculated from the estimated quaternion [13]. KF1 again shows a better angle estimation over the KF2 formulations. The errors of the KF1 and KF2 approaches have constant zero mean values over time. Better results of the KF2 formulation, which shows inferior positional and velocity results, are the consequence of good orientation constraints in the rotational joint and because the position vectors from the inertial units to the kinematic joint do not directly affect the orientation constraints in Eq. (54).

In the second step the estimation of the position vectors from the inertial units to the kinematic joints is discussed. Fig. 11 shows the absolute sum of all the position-vector errors. When using the adaptive approach the initial error value of 0.1704 meter decreases to a value of 0.0274 meter over approximately 100 iterations and stays constant or changes negligibly over the entire observation time. Considering the estimated and the reference position vectors in Eq. (47) the error vectors can be calculated:

$$\begin{aligned}
\Delta \bar{u}_1^{1,1} &= (0, -0.0002, 0.013)^T \text{ m}, & \Delta \bar{u}_2^{1,1} &= (0, -0.0004, 0.013)^T \text{ m}, \\
\Delta \bar{u}_1^{2,1} &= (0, 0.0018, -0.0123)^T \text{ m}, & \Delta \bar{u}_2^{2,1} &= (0, 0.0018, -0.0123)^T \text{ m}, \\
\Delta \bar{u}_1^{2,2} &= (-0.0017, -0.0011, 0.01)^T \text{ m}, & \Delta \bar{u}_2^{2,2} &= (-0.0017, -0.0011, 0.01)^T \text{ m}.
\end{aligned} \tag{58}$$

The deviations in the x and y -axis in the local frames show a negligible error, while the errors in the z -axis in the local frames deviate constantly by around 1 centimeter. These deviations can be related to the positioning and orientation of the inertial units on the rigid bodies with respect to the reference frame, because the motion is tightly restricted in the z -axis of the reference and local frames, but in practice there could be minor deviations. However, the rapid convergence of the position vectors from the inertial units to the kinematic joints is the consequence of the the adaptive approach, which adjust the initial covariance matrix Q_u toward the zero values with respect to the residual error of the observed position vectors.

The use of the adaptive approach with multiple inertial units on every rigid body might cause a problem with the observation of the state vector \mathbf{x}_{kin} in real time if there are many bodies in the system or if there are many constraint equations. For these reasons the approach with the multiple inertial units can only provide the calibration procedure for the estimation of the position vectors. On the other hand, when the position vectors from the inertial units to the kinematic joints converge, the redundant kinematic parameters in the state vector \mathbf{x}_{kin} and in the observation vector \mathbf{y} can be eliminated in a way that we observe the kinematic parameters with only one inertial unit on every rigid body.

In the last step the estimation of the sensors' bias vectors is discussed. Fig. 12 shows the estimation of the bias values on the selected axes of the accelerometer and the gyroscope. Despite the assumptions of the exponentially correlated change of the bias values, the figures show that the bias can also change because of the other influences, such as the change of the temperature or the internal changes in the sensors, which do not have the exponentially correlated stochastic behavior. The Kalman filter considers the estimation of the bias values with respect to the process and observation formulation.

5. Conclusion

In this study we present an approach to minimize the error of the kinematic parameters of a rigid body system due to the inaccurate positioning of the inertial units on the rigid body for the case when only the kinematic constraints are used for the correction of the inertial principle within the Kalman formulation. Based on the error propagation of the observation equations a general approach to the use of multiple inertial units on every rigid body is deduced if we are able to control the position vectors between the inertial units. The method was experimentally validated on a simple pendulum mechanism with the use of the minimum number of inertial units. We confirmed that the adaptive formulation gave better results than the standard formulation without an estimation of the position vectors from the inertial units to the kinematic joints.

The proposed approach has an advantage when we do not know the dynamics of the observed mechanism in advanced, because the independent and dependent parameters are observed simultaneously in the state vector. Therefore, this approach offers a quick solution in applications. On the other hand, we must be aware that increasing the number of rigid bodies in the system or possibly a larger number of inertial units can cause problems with the processing power. From the latter point of view this approach can represent a calibration procedure for the estimation of the position vector from the inertial units to the kinematic joints before the kinematic parameters are eventually observed.

The accuracy of the kinematic parameters when only the kinematic constraints are observed depends not only on the accurate positioning of the inertial units, but in general on the level of accuracy in the observation equations. A high level of noisy observation or a deviation from the assumed normally distributed noise can result in poorer performance or divergence of the Kalman filter. However, industrial mechanisms usually have well-defined constraints, and therefore the presented approach offers an appropriate alternative.

References

- [1] E. D. Roetenberg, P. J. Slycke, P. H. Veltink, Ambulatory position and orientation tracking fusing magnetic and inertial sensing, *IEEE Trans. on Bio. Eng.* 54 (2007) 883–890.
- [2] E. D. Roetenberg, C. T. M. Baten, P. H. Veltink, Estimating body segment orientation by applying inertial and magnetic sensing near ferromagnetic materials, *IEEE Trans. Neural. Sys. & Rehab. Eng.* 54 (2007) 883–890.
- [3] H. M. Schepers, E. D. Roetenberg, P. H. Veltink, Ambulatory human motion tracking by fusion of inertial and magnetic sensing with adaptive actuation, *Med. Bio. Eng. Comput.* 48 (2010) 27–37.
- [4] H. M. Schepers, P. H. Veltink, Stochastic magnetic measurement model for relative position and orientation estimation, *Meas. Sci. Technol.* 21 (2010).
- [5] M. Brodie, A. Walmsley, W. Page, Fusion motion capture: a prototype system using inertial measurement units and GPS for the biomechanical analysis of ski racing, *Sports Technology* 1 (2008) 17–28.
- [6] M. Supej, 3d measurements of alpine skiing with an inertial sensor motion capture suit and GNSS RTK system, *Journal of Sports Sciences* 28 (2010) 759–769.
- [7] I. Skog, P. Händel, In-car positioning and navigation technologies—a survey, *IEEE Transactions on Intelligent Transportation Systems* 10 (2009) 4–21.
- [8] J. D. Hol, T. B. Schön, H. J. Luinge, P. J. Slycke, F. Gustafsson, Robust real-time tracking by fusing measurement from inertial and vision sensors, *Journal of Real-Time Image Processing* 116 (2007) 266–271.
- [9] J. D. Hol, T. B. Schön, F. Gustafsson, Modeling and calibration of inertial and vision sensors, *International Journal of Robotics Research* 29 (2010) 231–244.
- [10] J. Youssef, B. Denis, C. Godin, S. Lesecq, Loosly-coupled IR-UWB handset and ankle-mounted inertial unit for indoor navigation, *International Journal of Robotics Research* 29 (2010) 231–244.
- [11] J. F. Wagner, Adapting the principle of integrated navigation systems to measuring the motion of rigid multibody systems, *Multibody System Dynamics* 1 (2004) 87–110.
- [12] P. Cheng, B. Oelmann, Joint-angle measurement using accelerometers and gyroscopes – a survey, *IEEE Transactions on Instrumentation and Measurement* 59 (2010) 404–414.
- [13] J. Kuipers, *Quaternions and Rotation Sequences*, Princeton University Press, 1999.
- [14] D. Choukroun, I. Y. Bar-Itzhack, Y. Oshman, Novel quaternion kalman filter, *IEEE Transactions on Aerospace and Electronic Systems* 42 (2006) 174–190.
- [15] D. W. Allan, Statistics of atomic frequency standards, *Proceedings of the IEEE* 54 (1966) 221–230.
- [16] D. W. Allan, Should the classical variance be used as a basic measure in standards metrology?, *IEEE Transactions on Instrumentation and Measurement* IM-36 (1987) 646–654.
- [17] IEEE Aerospace, E. S. Society, *IEEE standard specification format guide and test procedure for single-axis laser gyros*, IEEE Std 647–2006, 2006.
- [18] D. Gebre-Egziabher, R. C. Hayward, J. D. Powell, Design of multi-sensor attitude determination systems, *IEEE Transactions on Aerospace and Electronic Systems* 40 (2004) 627–649.
- [19] R. G. Brown, P. Y. C. Hwang, *Introduction to Random Signals and Applied Kalman Filtering*, John Wiley & Sons, Inc., 1997.
- [20] D.-J. Jwo, T.-S. Cho, Critical remarks on the linearised and extended kalman filters with geodetic navigation examples, *Measurements* 43 (2010) 1077–1089.
- [21] A. A. Shabana, *Computational dynamics*, A John Wiley & Sons, Inc., 1994.
- [22] I. Frosio, F. Pedersini, N. A. Borghese, Autocalibration of MEMS accelerometers, *IEEE Transactions on Instrumentation and Measurements* 58 (2009) 2034–2041.
- [23] Z. F. Syed, P. Aggarwal, C. Goodall, X. Niu, N. El-Sheimy, A new multi-position calibration method for MEMS inertial navigation system, *Measurement Science and Technology* 18 (2007) 1897–1907.

List of Figures

1	Observation of the arbitrary kinematic constraint with one inertial unit on each rigid body.	18
2	Observation of the arbitrary kinematic constraint with the arbitrary number of the inertial units on each rigid body.	19
3	Application of the proposed process and observation models within the Kalman-filtering formulation.	20
4	2-DoF pendulum.	21
5	2-DoF pendulum.	22
6	Inertial unit CH-6d and encoder positioning in the rotational joint.	23
7	Absolute angle in rotational joint with respect to the reference frame: a) first joint, b) second joint.	24
8	Absolute error of the position vector.	25
9	Absolute error of the velocity vector.	26
10	Error of the absolute angle around z^n -axis.	27
11	Sum of the absolute errors of the components of the position vectors from the inertial units to the kinematic joints.	28
12	Bias estimation.	29

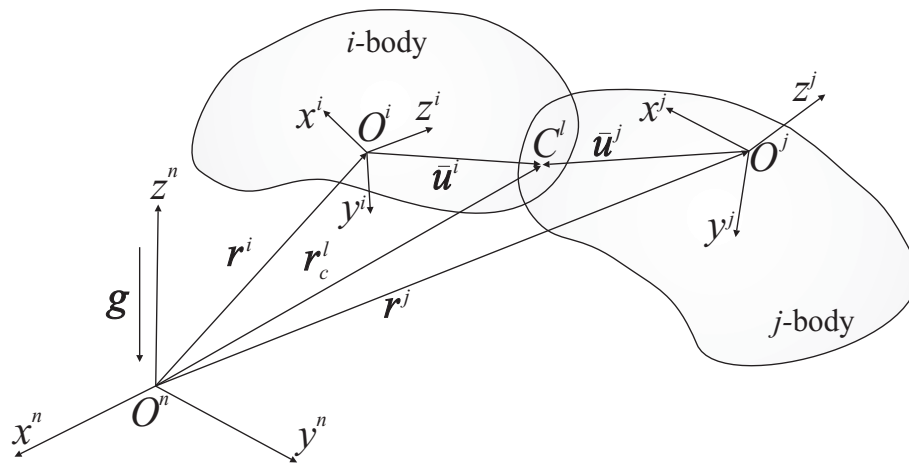


Figure 1: Observation of the arbitrary kinematic constraint with one inertial unit on each rigid body.

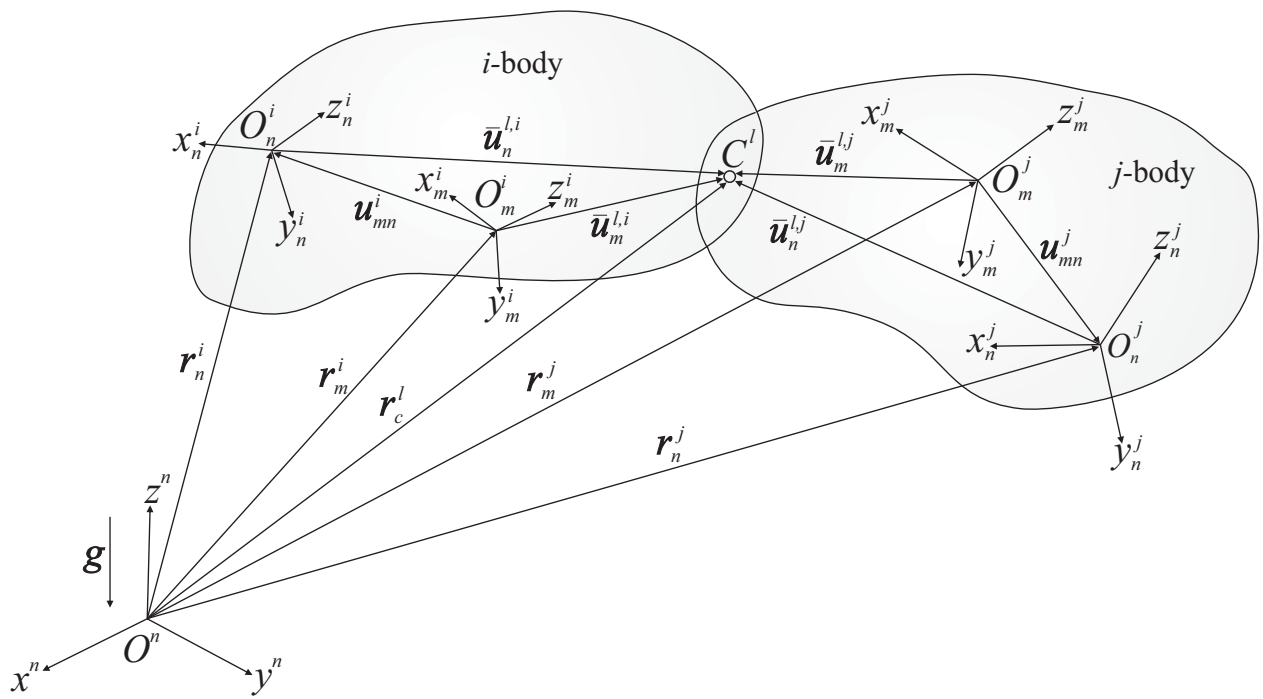


Figure 2: Observation of the arbitrary kinematic constraint with the arbitrary number of the inertial units on each rigid body.

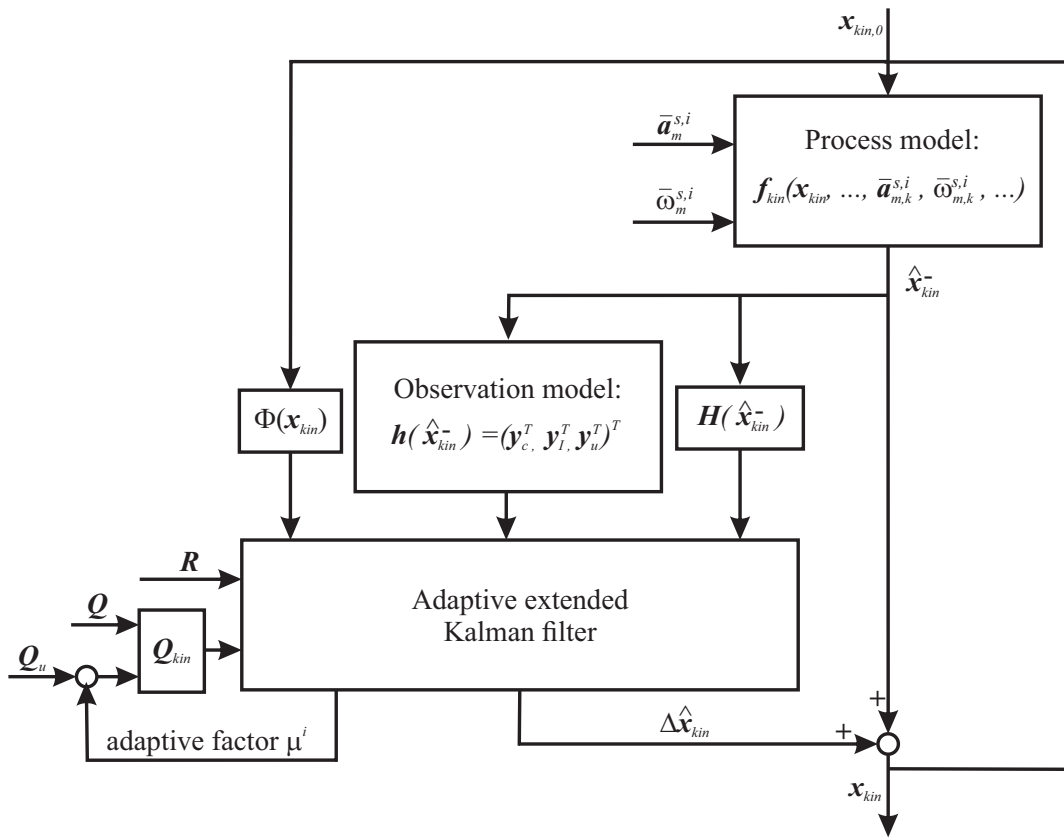
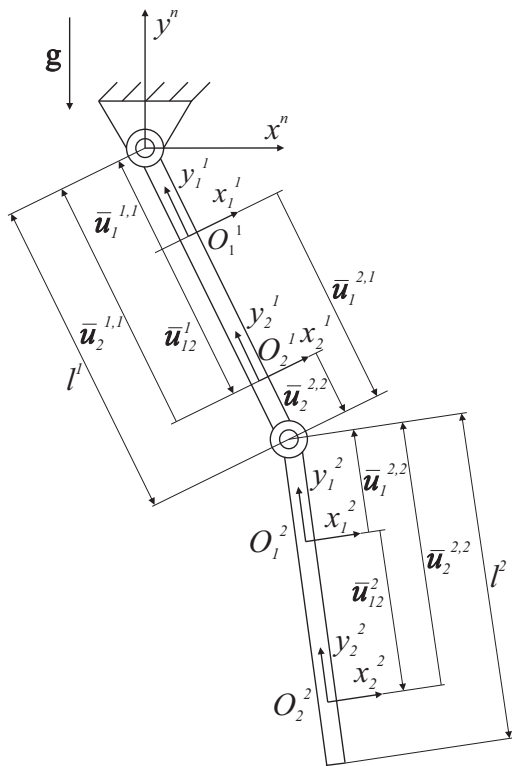
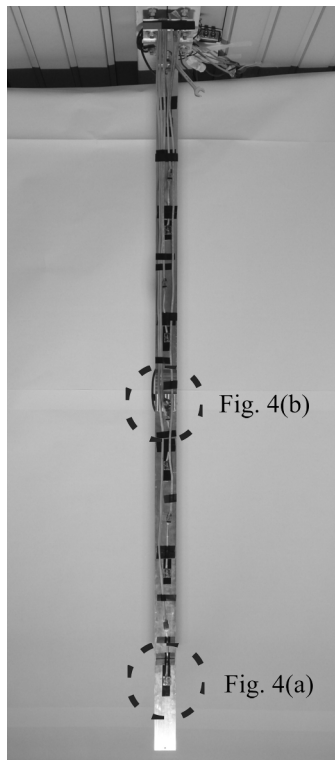


Figure 3: Application of the proposed process and observation models within the Kalman-filtering formulation.

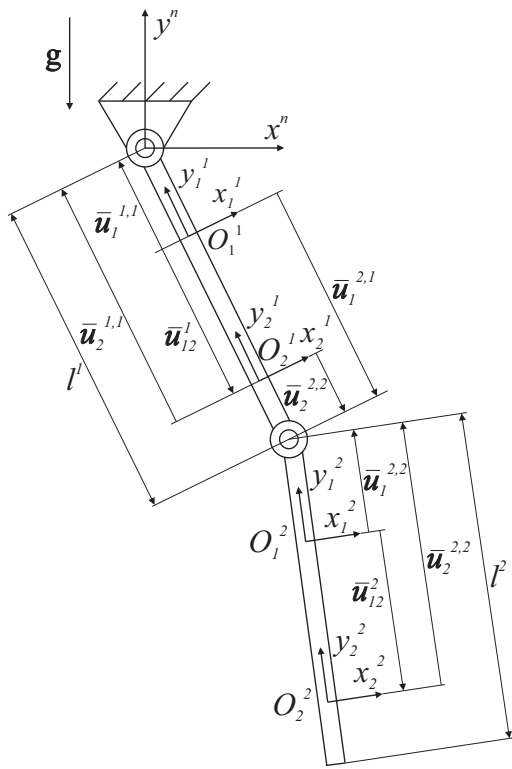


(a) Pendulum scheme.

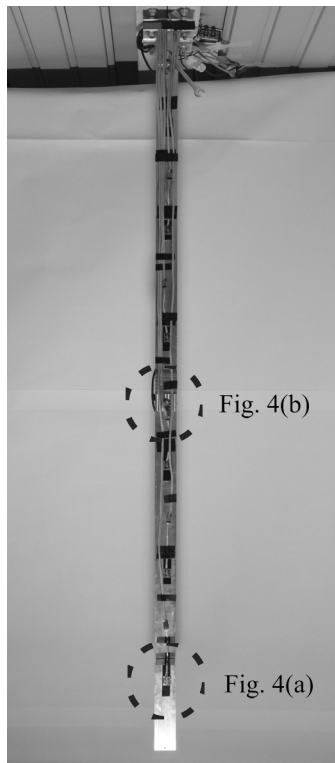


(b) Pendulum set-up in the laboratory.

Figure 4: 2-DoF pendulum.

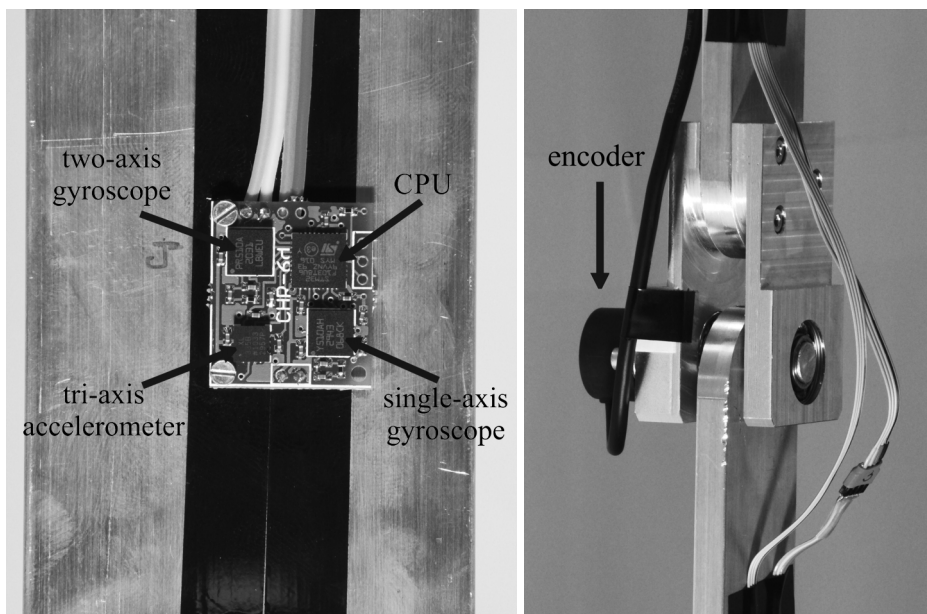


(a) Pendulum scheme.



(b) Pendulum set-up in the laboratory.

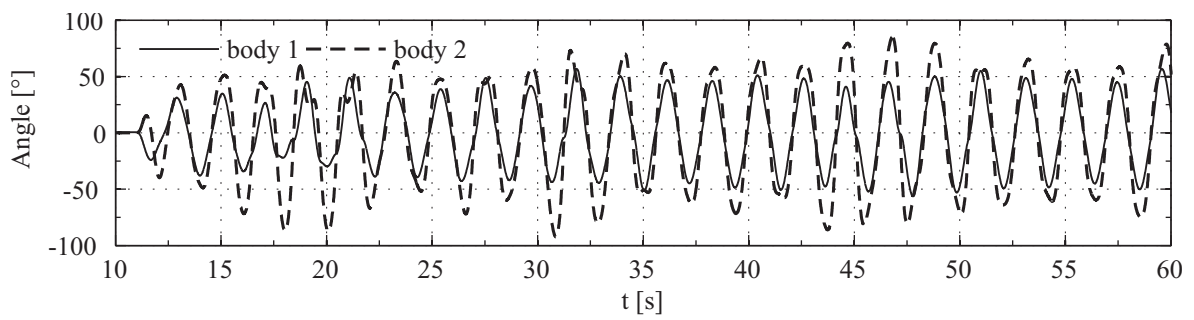
Figure 5: 2-DoF pendulum.



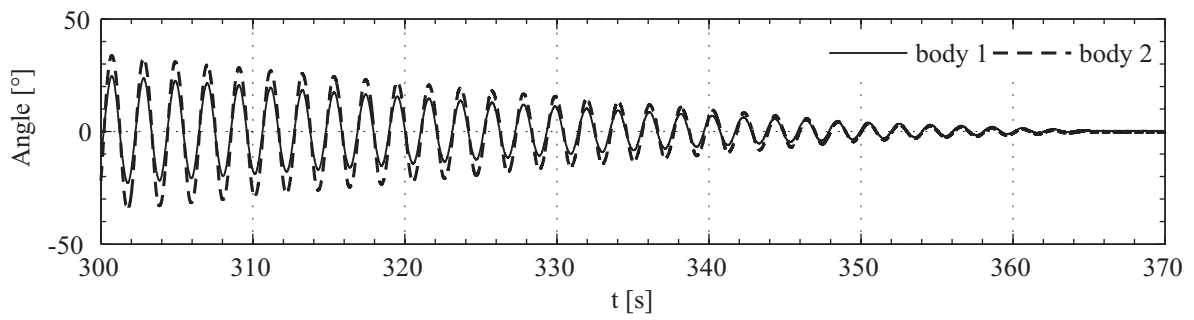
(a) Inertial unit CH-6d.

(b) Encoder fixing in the rotational joint between two rigid bodies.

Figure 6: Inertial unit CH-6d and encoder positioning in the rotational joint.

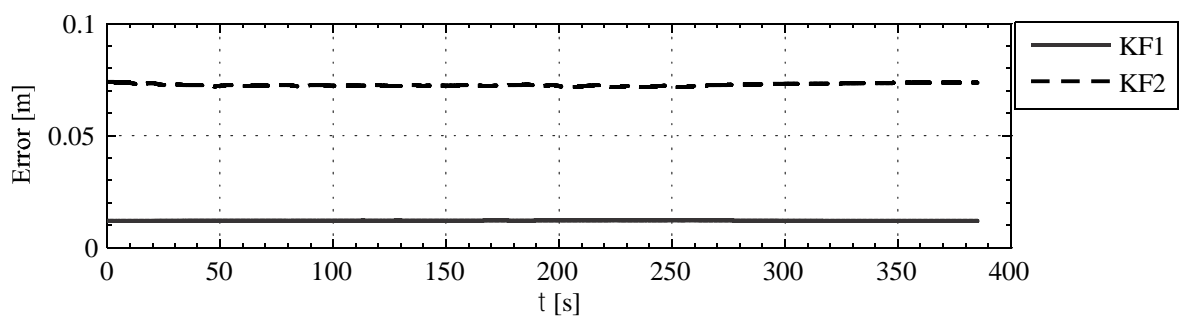


(a)

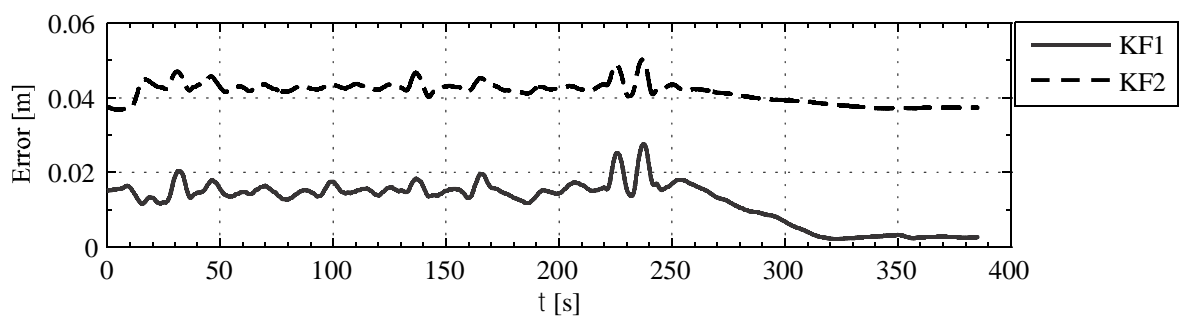


(b)

Figure 7: Absolute angle in rotational joint with respect to the reference frame: a) first joint, b) second joint.

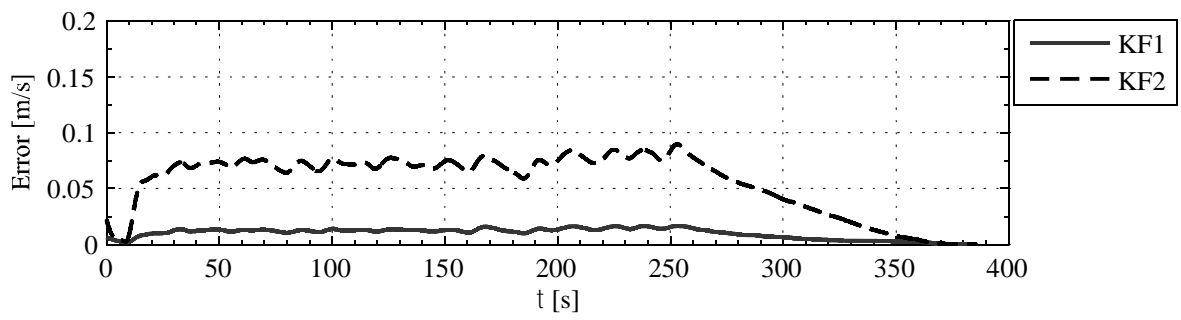


(a) r_1^1

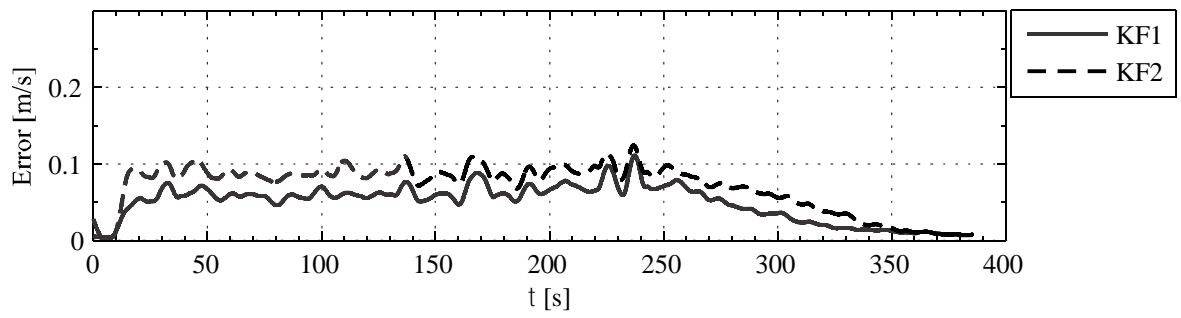


(b) r_2^2

Figure 8: Absolute error of the position vector.



(a) v_1^1



(b) v_2^2

Figure 9: Absolute error of the velocity vector.

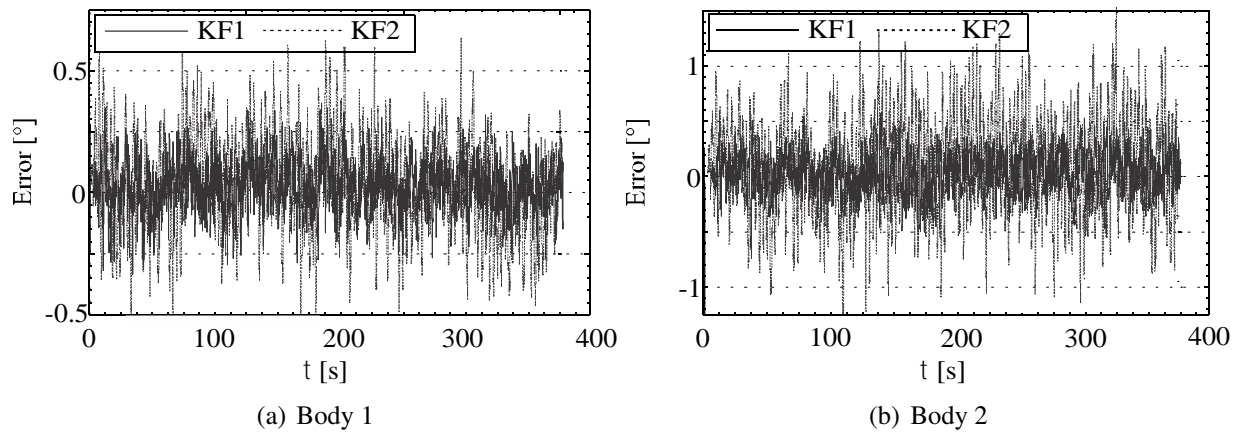


Figure 10: Error of the absolute angle around z^n -axis.

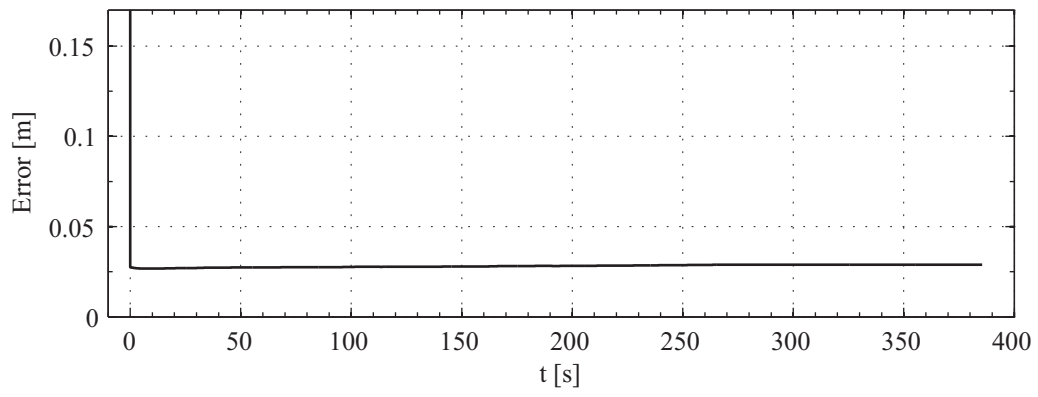
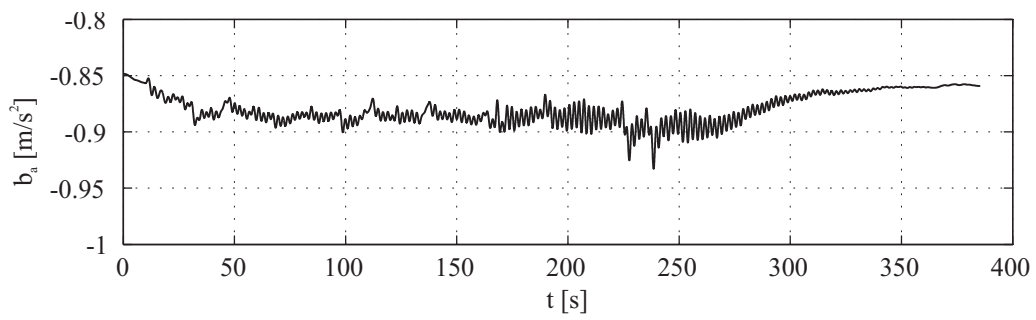
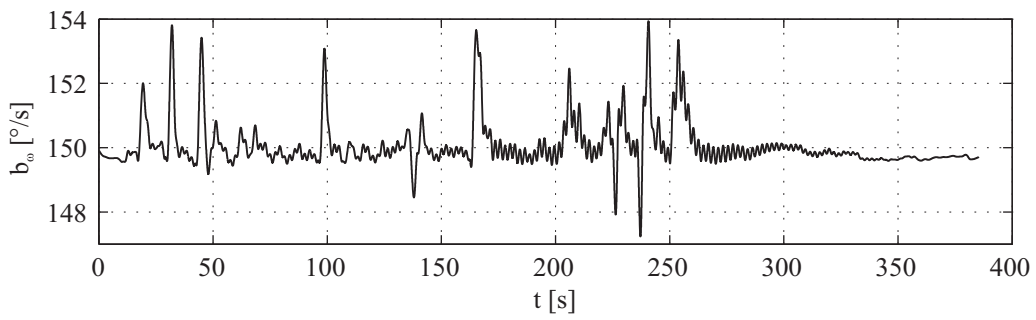


Figure 11: Sum of the absolute errors of the components of the position vectors from the inertial units to the kinematic joints.



(a) y-axis ADXL335 accelerometer (pos. I_1).



(b) z-axis LY510ALH gyroscope (pos. I_1).

Figure 12: Bias estimation.